

Microscopic theory of anomalous diffusion based on particle interactions

James F. Lutsko* and Jean Pierre Boon†

Physics Department, Code Postal 231, Université Libre de Bruxelles, 1050 Bruxelles, Belgium

(Received 22 February 2013; published 7 August 2013)

We present a master equation formulation based on a Markovian random walk model that exhibits subdiffusion, classical diffusion, and superdiffusion as a function of a single parameter. The nonclassical diffusive behavior is generated by allowing for interactions between a population of walkers. At the macroscopic level, this gives rise to a nonlinear Fokker-Planck equation. The diffusive behavior is reflected not only in the mean squared displacement [$\langle r^2(t) \rangle \sim t^\gamma$ with $0 < \gamma \leq 1.5$] but also in the existence of self-similar scaling solutions of the Fokker-Planck equation. We give a physical interpretation of sub- and superdiffusion in terms of the attractive and repulsive interactions between the diffusing particles and we discuss analytically the limiting values of the exponent γ . Simulations based on the master equation are shown to be in agreement with the analytical solutions of the nonlinear Fokker-Planck equation in all three diffusion regimes.

DOI: [10.1103/PhysRevE.88.022108](https://doi.org/10.1103/PhysRevE.88.022108)

PACS number(s): 05.40.Fb, 05.10.Gg, 05.60.-k

I. INTRODUCTION

Diffusion is a ubiquitous phenomenon observed in physical, chemical, biological, social, and algorithmic systems where “objects” (particles, molecules, cells, individuals, agents, etc.) move in a seemingly random sequence of steps in such a way that their mean squared displacement increases linearly in time: $\langle r^2 \rangle \sim t$ where the proportionality factor is a constant which (apart from a numerical factor) is the diffusion coefficient. The resulting effect is a spread of the spatial distribution of the objects in the form of a Gaussian whose width grows with the square root of time. A microscopic mechanism yielding diffusive behavior at the macroscopic scale is based on the simple model of point particles undergoing random displacements on a one-dimensional lattice where they hop left or right from site to site at each tick of the clock: this is the random walk model for Brownian particle diffusion designed by Einstein who in 1905 formulated the first microscopic derivation of the diffusion equation [1].

However, there are many instances where the “objects” do not move freely: obstacles, time delays, interactions can modify their trajectories in such a way that the mean squared displacement deviates from the linear law and the Gaussian structure of the dispersion is deformed or replaced by a different distribution. So more generally, one observes $\langle r^2 \rangle \sim t^\gamma$ where for normal diffusion $\gamma = 1$ while if $\gamma \neq 1$ one talks about *anomalous diffusion*: when $\gamma < 1$ the process is said to be *subdiffusive* and when $\gamma > 1$ it is *superdiffusive*. As a result, there has been considerable interest in developing stochastic models capable of generating such behavior and the difficulty in constructing models depends on the requirements imposed. The most fundamental constraint is, of course, the need to reproduce a mean squared displacement that exhibits power-law behavior as a function of time but this is a rather weak constraint that can be fulfilled in many ways. Perhaps the strongest demand that can be made is for the existence of self-similar solutions which is equivalent to demanding that *all* moments scale similarly, $\langle r^{2n} \rangle \sim t^{n\gamma}$. This implies that the

distribution has the form $f(r,t) = t^{-\gamma/2} \phi(r/t^{\gamma/2})$ for some function $\phi(x)$ which is the case for classical diffusion. Another characteristic of classical diffusion is a type of universality wherein the details of the microscopic model can be changed without affecting the macroscopic process. In the Einstein model, the jumps can be of lengths greater than 1 with different probabilities including rests (jumps of length zero) without affecting the process (and, indeed, with the same diffusion constant). More generally, diverse microscopic dynamics can give rise to “diffusion” at the macroscopic level, but the underlying mechanisms may be quite different; for instance the distinction should be made between tracer motion where experimentally one follows trajectories of distinguishable particles seeded in an active medium [2,3] and the motion of tagged particles which, while identical to the medium particles, are made observable by radioactive or fluorescent markers [4]. The latter case is referred to as molecular diffusion, which is the dynamical process considered here.

One class of diffusion models involves the use of memory or, equivalently, correlated noise since it is easy to see that if in two successive steps, a random walker preferentially follows the first step with one in the same direction (or the opposite direction) the rate of diffusion can be dramatically altered. Non-Markovian dynamics is the mechanism behind the fractional Brownian motion [5,6] and certain lattice models such as the elephant random walk [7,8]. Similarly, the use of correlated noise in the generalized Langevin equation [9] leads to the fractional Fokker-Planck equation [10] describing the phenomenology of anomalous diffusion in large ensembles [11] and for single trajectories [12].

One might wonder whether a Markovian random walk can give rise to anomalous diffusion. It is probably the case that *any* type of scaling of the mean squared displacement is possible via the application of an external force (which is to say, jump probabilities or waiting times that depend on spatial position) but the existence of a field obviously corresponds to a very particular physical circumstance. Recently, we showed that subdiffusive behavior could also be realized in a random walk model in which the walkers interact with one another [13,14] and which is indeed Markovian and contains no external force. Starting with a rather general ansatz for the way in which interactions affect the probability of jumps we derived from

*jlutsko@ulb.ac.be; <http://www.lutsko.com>†jpbtoon@ulb.ac.be; <http://homepages.ulb.ac.be/~jpbtoon/>

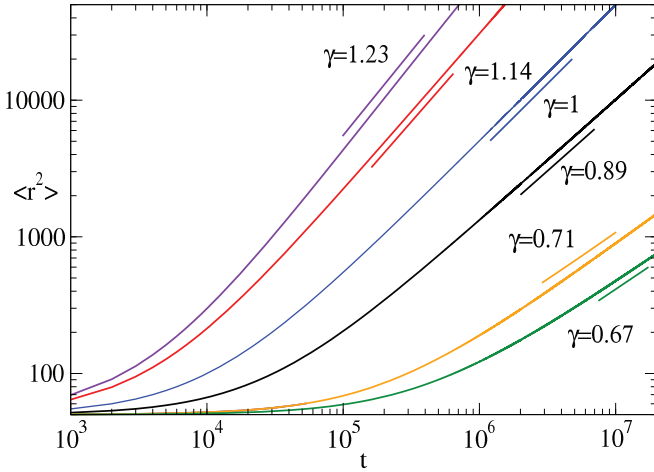


FIG. 1. (Color online) The mean squared displacement as a function of time obtained from the solutions of the master equation for the cases of sub-, classical, and superdiffusion with a Gaussian initial condition. Other details of the simulation are described in Sec. IV. Only a single parameter varied is varied, α in Eq. (19), and the scaling exponents are predicted from the generalized diffusion equation (6), to be $\gamma = 2/(\alpha + 1)$. The line segments are curves of the form $\langle r^2 \rangle = at^\gamma$ and verify the diffusive scaling with the predicted exponents at long times. In this figure the mean squared displacement is given in units of lattice spacings δr and the time in units of the fixed jump time δt .

the master equation, via a multiscale expansion, a nonlinear Fokker-Planck equation, a generalization of the so-called porous medium equation. When this was combined with the requirement for diffusivelike self-similar solutions, it was shown that certain limits of the jump probabilities (as explained in detail below) had to depend on the concentration of walkers in a specific power-law form. The resulting description of subdiffusion was quite different from that given by non-Markovian models. For example, the fractional Fokker-Planck equation leads to a stretched-exponential distribution while the nonlinear model gives algebraic power-law distributions. This approach was also extended to the description of nonlinear reaction-diffusion systems [15].

In this paper, we further extend our previous work to include a description of superdiffusion. Indeed, we show that the same microscopic random walk model can exhibit subdiffusion, classical diffusion, and superdiffusion at the macroscopic scale as illustrated in Fig. 1 simply by varying a single parameter. In all cases, the behavior is “diffusive” in the strong sense of allowing for self-similar solutions. It will also be apparent that the model shows a kind of universality in which different microscopic dynamics yield the same macroscopic behavior. The ingredients needed to give this range of behavior are both nonlinearity and (spatial) nonlocality. While our previous work showed that nonlinearity alone was sufficient to give rise to subdiffusion, we find that spatial nonlocality is critical to achieve superdiffusion within our framework. In some sense, this might be thought of as a complement or dual to the temporal nonlocality of the non-Markovian approaches.

In the next section, we review our formalism and apply it to a particular form of nonlocal interaction between walkers. In Sec. III, we present direct numerical solutions of the master

equation and compare to the predictions of the macroscopic nonlinear Fokker-Planck equation. We show that in the superdiffusive case, considerable care is needed in extracting the continuum limit from microscopic simulations but that the two are indeed in agreement. The paper concludes with a few comments on our results.

II. RANDOM WALK MODEL AND NONLINEAR FOKKER-PLANCK EQUATION

A. The master equation

Consider a walker moving on a one-dimensional lattice whose sites are labeled by integers $j = \dots, -2, -1, 0, 1, 2, \dots$. The formal expression of the microscopic dynamics describing the diffusive motion of Einstein’s random walk model reads

$$n^*(r; t + 1) = \xi^{(-1)} n^*(r + 1; t) + \xi^{(+1)} n^*(r - 1; t), \quad (1)$$

where the Boolean variable $n^*(r; t) = \{0, 1\}$ denotes the occupation at time t of the site located at position r and $\xi^{(\pm 1)}$ is a Boolean random variable controlling the particle jump between neighboring sites ($\xi^{(-1)} + \xi^{(+1)} = 1$); the superscript index (± 1) indicates specifically that the jumps occur over one lattice distance. Extending the possible jump steps over the whole lattice, Eq. (1) becomes

$$n^*(r; t + 1) = \sum_{j=-\infty}^{+\infty} \xi^{(j)} n^*(r - j; t), \quad (2)$$

with $\sum_{j=-\infty}^{+\infty} \xi^{(j)} = 1$ (which condition prevents conflicting occupations at the arrival site).

The mean field description follows by ensemble averaging Eq. (2) with $\langle n^*(r; t) \rangle = f(r; t)$ and $\langle \xi^{(j)} \rangle = P_j$, where j is the position index; using statistical independence of the ξ ’s and n^* , we obtain

$$f(r; t + \delta t) = \sum_{j=-\infty}^{+\infty} P_j f(r - j\delta r; t), \quad (3)$$

where the distance, in lattice units, between neighboring sites is denoted by δr and $P_j(\ell)$ is the probability of a jump of j sites from site ℓ with $\sum_j P_j(\ell) = 1$. Setting $j = \pm 1$ and $P_{\pm 1} = 1/2$ in Eq. (3), we have the master equation for the usual random walk from which Einstein derived the classical diffusion equation [1]. Note that Eq. (3) can also be rewritten as

$$\begin{aligned} f(r, t + \delta t) - f(r, t) \\ = \sum_j [P_j(r - j\delta r) f(r - j\delta r, t) - P_j(r) f(r, t)], \end{aligned} \quad (4)$$

which expresses the rate of change of the particle distribution as the difference between the incoming and outgoing fluxes at location r . Equation (3) generalizes Einstein’s master equation, providing a formulation which in the hydrodynamic limit leads to the description of nonclassical diffusion: when $P_j(\ell)$ has a functional form $p_j F[f(r, t)] \sim p_j f^{\alpha-1}$ (where p_j is a prescribed spatial distribution), Eq. (3) becomes the master equation leading to the description of nonlinear diffusion [13].

B. The Fokker-Planck equation

We now introduce the further generalization that the jump probabilities $P_j(\ell)$ take a functional form depending on both concentrations at the starting point and at the end point of the jump:

$$P_j = p_j F[f(r - j \delta r, t), f(r, t)] \quad \text{with} \quad \sum_j P_j = 1, \quad (5)$$

where the probabilities p_j are drawn from a prescribed distribution and the bounding condition $0 \leq P_j \leq 1$ imposes $0 \leq F(x, y) \leq 1$ as well as restrictions on the functional form of $F(x, y)$. Under these conditions, multiscale expansion of the master equation was shown to give the generalized Fokker-Planck (or generalized diffusion) equation [14]

$$\begin{aligned} \frac{\partial f}{\partial t} + C \frac{\partial}{\partial r} [x F(x, x)]_f \\ = D \frac{\partial}{\partial r} \left[\frac{\partial x F(x, y)}{\partial x} - \frac{\partial x F(x, y)}{\partial y} \right]_f \frac{\partial f}{\partial r} \\ + \frac{1}{2} C^2 \delta t \frac{\partial}{\partial r} \left[\frac{\partial x F(x, y)}{\partial x} - \frac{\partial x F(x, y)}{\partial y} \right. \\ \left. - \left(\frac{\partial x F(x, x)}{\partial x} \right)^2 \right]_f \frac{\partial f}{\partial r}, \end{aligned} \quad (6)$$

with the notation

$$\left[\frac{\partial x F(x, y)}{\partial x} \right]_f = \left[\frac{\partial x F(x, y)}{\partial x} \right]_{x=f(r, t), y=f(r, t)}. \quad (7)$$

In Eq. (6), C and D are respectively the drift velocity and the diffusion coefficient,

$$\begin{aligned} C &= \frac{\delta r}{\delta t} \sum_j j p_j = \frac{\delta r}{\delta t} J_1, \\ D &= \frac{1}{2} \frac{(\delta r)^2}{\delta t} \left[\left(\sum_j j^2 p_j \right) - J_1^2 \right] = \frac{1}{2} \frac{(\delta r)^2}{\delta t} (J_2 - J_1^2), \end{aligned} \quad (8)$$

where the J_n 's denote the moments $J_n = \sum_j j^n p_j$. We assume throughout that the constants p_j are probabilities so that they satisfy $0 \leq p_j \leq 1$ and that their sum is equal to 1. Otherwise, they are arbitrary except for the condition that the first and second moments, Eq. (8) above, be finite. Note that for $F(x, y) = 1$, Eq. (6) reduces to the classical advection-diffusion equation.

Since the function $F(x, y)$ is defined in terms of the jump probabilities, it must be bounded, and so must satisfy

$$0 \leq x F(x, y) \leq 1 \quad \text{and} \quad 0 \leq y F(x, y) \leq 1, \quad \forall x, y \in [0, 1]. \quad (9)$$

It was shown in [14] that self-similar solutions are possible if and only if

$$\lim_{y \rightarrow x} \left[\frac{\partial x F(x, y)}{\partial x} - \frac{\partial x F(x, y)}{\partial y} \right] \sim x^{\alpha-1}, \quad (10)$$

where the scaling exponent α is related to the diffusion exponent by

$$\gamma = \frac{2}{\alpha + 1}. \quad (11)$$

Our previous work focused on *local* models for which $F(x, y) \equiv F(x)$, in which case the bounds given above (9) demand that $\alpha \geq 1$ and therefore $0 \leq \gamma \leq 1$, which is the correct formulation of subdiffusion [16] but excludes the case of superdiffusion ($\gamma > 1 \iff \alpha < 1$).

III. SUBDIFFUSION AND SUPERDIFFUSION

A. A model for sub- and superdiffusion

Both types of anomalous diffusion (sub- and superdiffusion) can be described in a single formulation when the jump probabilities depend on the occupation probabilities at both the starting point and the end point of the jump by means of the ansatz

$$F(x, y; \omega_s, \omega_e) \sim \omega_s F_s(x) + \omega_e F_e(y), \quad (12)$$

where ω_s and ω_e are weighting factors relative to the functionals of the concentrations at the starting point and at the end point of the jump. Since an overall scale factor is unimportant, we can divide by ω_s and write $a \equiv \omega_e/\omega_s$ without loss of generality. Finally, in order to assure that the constraint (9) is satisfied, we normalize to give the ansatz

$$F(x, y; a) = \frac{F(x) + a F(y)}{F(x) + F(y)}. \quad (13)$$

The positivity arguments x, y and the constraints (9) and $F(x, y; a) \geq 0$ imply that $0 \leq a \leq 1$. We emphasize that this ansatz is motivated by simplicity and the necessary mathematical requirements.

Considering the case that there is no drift [$C = 0$ in Eq. (6)], and in order that the general formulation describe diffusion, we should have a scaling solution of the form $f(r, t) = t^{-\gamma/2} \phi(r/t^{\gamma/2})$; it was shown in [14] that the scaling hypothesis demands that

$$\lim_{y \rightarrow x} \left(\frac{\partial}{\partial x} x F(x, y; a) - \frac{\partial}{\partial y} x F(x, y; a, \alpha) \right) = K x^{\alpha-1} \quad (14)$$

for some constant α . Using the model functional (13) in the left-hand side (LHS) of (14) gives

$$\frac{1+a}{2} + \frac{1-a}{2} \frac{x F'(x, a, \alpha)}{F(x; a, \alpha)} = K x^{\alpha-1}, \quad (15)$$

which is solved to yield

$$F(x; a, \alpha) = \frac{B}{x^{(1+a)/(1-a)}} \exp\left(\frac{2K}{1-a} \frac{x^{\alpha-1}}{\alpha-1}\right), \quad (16)$$

where B is an integration constant; reinserting (16) into (13), we find

$$F(x, y; a, \alpha) = \frac{1+a \left(\frac{x}{y}\right)^{(1+a)/(1-a)} \exp\left(\frac{2K}{1-a} \frac{y^{\alpha-1} - x^{\alpha-1}}{\alpha-1}\right)}{1 + \left(\frac{x}{y}\right)^{(1+a)/(1-a)} \exp\left(\frac{2K}{1-a} \frac{y^{\alpha-1} - x^{\alpha-1}}{\alpha-1}\right)}. \quad (17)$$

The natural limit $\lim_{\alpha \rightarrow 1} F(x, y; a) = 1$ requires $K = \frac{1}{2}(1+a)\bar{K}^{\alpha-1}$ where \bar{K} is an arbitrary constant with units of length. Thus,

$$F(x, y; a, \alpha) = \frac{1 + a G(x, y; a, \alpha)}{1 + G(x, y; a, \alpha)}, \quad (18)$$

with

$$G(x, y; a, \alpha) = \left(\frac{x}{y}\right)^{(1+a)/(1-a)} \exp\left(\frac{1+a}{1-a} \frac{\bar{K}^{\alpha-1} y^{\alpha-1} - x^{\alpha-1}}{\alpha-1}\right). \quad (19)$$

It is clear that the limits $a = 1$ and $\alpha \rightarrow 1$ give normal diffusion [$F(x, y; a, \alpha) = 1$] and, for any finite value of $x > 0$, we have $0 \leq F(x, y; a, \alpha) < 1, \forall y \in [0, 1]$. Furthermore, one has that

$$\begin{aligned} \lim_{x \rightarrow 0} F(x, y; a, \alpha) &= \begin{cases} 1, & \alpha > 1, \\ a, & \alpha < 1, \end{cases} \quad \text{and} \\ \lim_{y \rightarrow 0} F(x, y; a, \alpha) &= \begin{cases} a, & \alpha > 1, \\ 1, & \alpha < 1. \end{cases} \end{aligned} \quad (20)$$

To provide some interpretation for this model, we note that

$$\begin{aligned} \frac{\partial}{\partial x} F(x, y; a, \alpha) &= (1+a) \frac{G(x, y; a, \alpha)}{[1 + G(x, y; a, \alpha)]^2} \left(\frac{(\bar{K}x)^{\alpha-1} - 1}{x}\right), \quad (21) \end{aligned}$$

$$\begin{aligned} \frac{\partial}{\partial y} F(x, y; a, \alpha) &= (1+a) \frac{G(x, y; a, \alpha)}{[1 + G(x, y; a, \alpha)]^2} \left(\frac{1 - (\bar{K}y)^{\alpha-1}}{y}\right). \quad (22) \end{aligned}$$

Since $0 < x, y < 1$, the signs of these derivatives are determined by the factors on the right: $[(\bar{K}x)^{\alpha-1} - 1]$ and $[1 - (\bar{K}y)^{\alpha-1}]$, and so depend on whether $(\alpha - 1)$ is positive or negative:

$$\begin{aligned} \alpha > 1 &\implies \frac{\partial}{\partial x} F(x, y; a, \alpha) < 0 < \frac{\partial}{\partial y} F(x, y; a, \alpha), \\ \alpha < 1 &\implies \frac{\partial}{\partial x} F(x, y; a, \alpha) > 0 > \frac{\partial}{\partial y} F(x, y; a, \alpha). \end{aligned} \quad (23)$$

In the first case, $\alpha > 1$, the jump probability decreases with the concentration at the starting point and increases with the concentration at the arrival site; in other words the jump rate is reduced by putting more walkers at the origin and increased by putting more at the terminus of a jump: this is analogous to an attractive interaction. For $\alpha < 1$, we have the reverse situation: the jump rate is increased by putting more walkers at the origin and decreased by putting more at the terminus, thus emulating a repulsive interaction. In the standard problem with all walkers at the origin at $t = 0$, the distribution decays monotonically away from the origin; thus, if the particles repel, the distribution expands faster (i.e., tends to a uniform distribution more quickly) whereas if they attract, then this attraction slows down the spread of the distribution. The physical interpretation is that attractive interactions give subdiffusion and repulsive interactions give superdiffusion.

B. Explicit form of the scaling solutions

In the absence of drift, the generalized advection-diffusion equation (6) with (18) and (19) reads

$$\frac{\partial f}{\partial t} = \bar{K}^{\alpha-1} \frac{1+a}{2\alpha} D \frac{\partial^2}{\partial r^2} f^\alpha, \quad (24)$$

and the scaling solutions are obtained following the development given in Ref. [14], yielding

$$f(r, t) = t^{-\gamma/2} W \left(1 \pm V \frac{r^2}{t^\gamma}\right)^{1/(\alpha-1)}, \quad (25)$$

where W will be determined by normalization. Inserting (25) into (24) gives [with (11)]

$$V W^{\alpha-1} = \bar{K}^{1-\alpha} \frac{|1-\alpha|}{1+\alpha} \frac{1}{1+a} D^{-1}. \quad (26)$$

(i) For the superdiffusive case, $\alpha < 1$,

$$f(r, t) = t^{-\gamma/2} W \left(1 + V \frac{r^2}{t^\gamma}\right)^{1/(\alpha-1)}. \quad (27)$$

The normalization condition (using the reduced variable $\zeta = V^{1/2} \frac{r}{t^{\gamma/2}}$) reads

$$W V^{-1/2} \int_{-\infty}^{\infty} d\zeta (1 + \zeta^2)^{1/(\alpha-1)} = 1,$$

where the integral exists (is finite) provided

$$\frac{\alpha+1}{\alpha-1} < 0 \implies \alpha > -1 \implies \gamma > 1, \quad (28)$$

and the mean squared displacement $\langle r^2 \rangle = \int_{-\infty}^{\infty} r^2 f(r; t) dr$ is given by

$$\langle r^2 \rangle = t^\gamma W V^{-3/2} \int_{-\infty}^{\infty} d\zeta \zeta^2 (1 + \zeta^2)^{1/(\alpha-1)},$$

and will be finite only if

$$\frac{3\alpha-1}{\alpha-1} < 0 \implies \alpha > \frac{1}{3} \implies \gamma < \frac{3}{2}. \quad (29)$$

(ii) For the subdiffusive case, $\alpha > 1$, the distribution has finite support so that

$$f(r, t) = t^{-\gamma/2} W \left(1 - V \frac{r^2}{t^\gamma}\right)^{1/(\alpha-1)} \Theta\left(1 - V \frac{r^2}{t^\gamma}\right), \quad (30)$$

with the normalization condition

$$W V^{-1/2} \int_{-1}^1 d\zeta (1 - \zeta^2)^{1/(\alpha-1)} = 1,$$

and the mean squared displacement

$$\langle r^2 \rangle = t^\gamma W V^{-3/2} \int_{-1}^1 d\zeta \zeta^2 (1 - \zeta^2)^{1/(\alpha-1)}.$$

The continuum results therefore imply that an initial distribution of the form $W'[1 + s_\alpha(r/w)^2]^{1/(\alpha-1)} \Theta[1 + s_\alpha(r/w)^2]$, with W' determined by normalization and $s_\alpha = \mp$ for $\alpha \gtrless 1$, will evolve self-similarly with mean squared displacement increasing as t^γ . Indeed for both sub- and superdiffusion, the mean squared displacement takes the form

$$\langle r^2 \rangle = \tilde{D} t^\gamma, \quad (31)$$

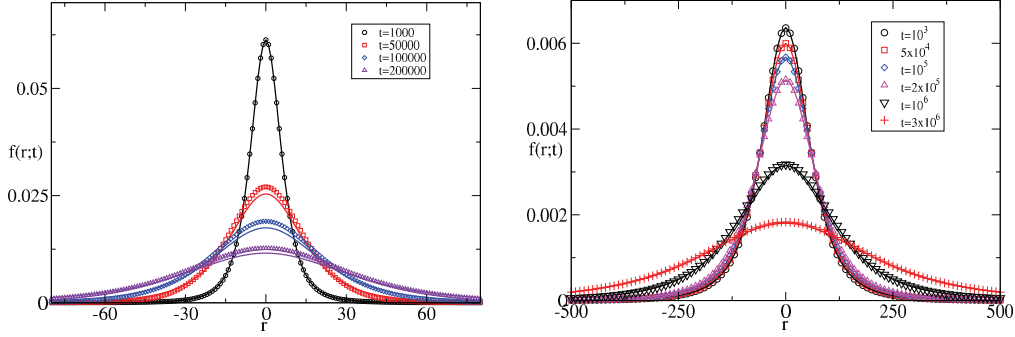


FIG. 2. (Color online) The spatial distribution as a function of time as determined by direct numerical solution of the master equation (symbols) and the analytic distribution, Eq. (30) for the case $\alpha = 0.5$ corresponding to a scaling exponent of $\gamma = 4/3$. All quantities are dimensionless (i.e., $\delta r = \delta t = 1$). In both cases, the initial distribution was the predicted scaling solution as described in the text: for the figure on the left, the initial width was $w = 10$ while for the figure on the right it was $w = 100$.

with

$$\tilde{D} = \text{const} \times W V^{-3/2} = \text{const} \times \bar{K}^{\gamma(\alpha-1)} \left(\frac{2}{\gamma} \frac{1+a}{1-\alpha} \right)^{\gamma} D^{\gamma}. \quad (32)$$

Note that, while D has the usual dimensions of a diffusion coefficient, $[\tilde{D}] = L^2 T^{-\gamma}$.

IV. NUMERICAL SIMULATIONS

A. Comparison between the master equation and the nonlinear Fokker-Planck equation

Because the macroscopic description (the nonlinear Fokker-Planck equation) is derived from the microscopic dynamics (i.e., the random walk model) by means of a well-defined but approximate multiscale expansion it is interesting to compare the two to verify that they are indeed in agreement for the ansatz proposed here. We therefore wish to compare the result of the direct, numerical, solution of the master equation to the continuum model, the generalized diffusion equation (24), which predicts the existence of exact scaling solutions (the explicit forms of which are given in Sec. III B).

In the following, we use the elementary probabilities $p_{\pm i} = p$ for $1 \leq i \leq n$ for some values of p and n and have set $a = 0$. Following our previous work [14], we will use $n = 2$ (although in fact we have obtained similar results for one-step jumps, $n = 1$). We found that the simulations were increasingly sensitive to the value of p as α decreased: in fact, when this parameter is too large, and when $\alpha < 1$ (superdiffusive case) the distribution determined from the master equation does not decay smoothly but, rather, shows an oscillatory structure in both space and time with a spatial period of several lattice sites. This is because in this case the walkers repel each other. So, if in an initial configuration the probability satisfies $f_n > f_{n+1}$ then so much more probability can get transferred from site n to site $n+1$ than is transferred from $n+1$ to $n+2$ that one finds $f_{n+1} > f_n$. In the next time step, this causes a flow in the opposite direction. We therefore fixed on a value of $p = 10^{-4}$ which is small enough to avoid any lattice-scale oscillatory behavior for $\alpha \geq 0.5$ although we could use, e.g., $p = 10^{-3}$ for $\alpha \geq 0.75$.

Even with this problem under control, we did not immediately obtain agreement between the lattice and continuum

models. The left panel of Fig. 2 shows several snapshots of the distribution for the case $\alpha = 0.5$ ($\gamma = 4/3$) starting with a distribution of width $w = 10$. While the two distributions are similar, there are significant differences between them. This was reflected in the mean squared displacement from a run of 1×10^6 updates of the master equation which appeared to behave as a power law but with an exponent γ of approximately 1.5 which is considerably larger than expected. Trying a wider initial distribution improved the agreement with the theoretical distribution (see Fig. 2; right panel) but still gave an exponent of about 1.45 for the mean squared displacement. In order to test whether this is an equilibration effect, we used runs of 10×10^6 time steps and extracted the mean squared displacement from each window of 1×10^6 steps: the results are shown in Fig. 3. It is clear that several million time steps are required for the exponent of the mean squared displacement to stabilize but even then, the final value is significantly above the theoretical value. Finally, in Fig. 4, we show the long-time value (from the final window of 1×10^6 updates) as a function of the initial width of the distribution. Fitting to a function of the form $\gamma(w) = \gamma_{\infty} + a(\frac{1}{w})^b$ gives for $\alpha = 0.5$ a value of $\gamma_{\infty} = 1.34$ and for $\alpha = 0.65$ a value of $\gamma_{\infty} = 1.23$, which compare well with the theoretical values of 1.33 and 1.21, respectively.

Why should the result be so sensitive to the width of the distribution? Note that in order to obtain the continuum limit, we have to expand the distribution $f(x+n)$ in terms of $f(x)$. However, the form of the jump probability actually requires that we evaluate terms of the form

$$f^{(\alpha-1)}(x+n) - f^{(\alpha-1)}(x) = (\alpha-1)f^{\alpha-2}(x)f'(x)n + \dots$$

The point is that with $\alpha < 1$, and given that $f(x) < 1$, the coefficient $f^{\alpha-2}(x)$ can be very large so that the expansion is only reasonable if $f'(x)$ is sufficiently small which, in turn, requires a wide enough distribution in units of lattice spacing.

In summary, to get agreement with the continuum limit for the smallest values of α considered here—which is to say, for the strongest superdiffusivity—it is necessary to begin with very wide distributions and to perform sufficiently long runs. However, it is important to emphasize that these statements are quantified in terms of lattice spacings and time steps: this has nothing to do with the *physical* width of the distribution and the *physical* duration of the process since both of these depend on the, as yet unspecified, δr and δt . As the distribution

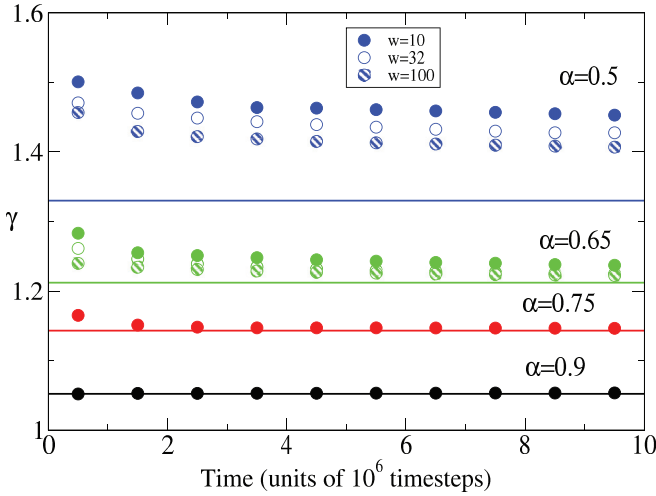


FIG. 3. (Color online) The scaling exponent γ as determined from fits of the numerical solution of the master equation. The fits were to the predicted functional form $\langle r^2 \rangle = a_0(a_1 + t)^\gamma$ and were performed independently with successive windows of 10^6 time steps. The figure also shows results for different initial widths w (in units of lattice spacings) as described in the text. The lines are drawn at the predicted values $\gamma = 2/(1 + \alpha)$.

becomes wider and the times become longer, we can decrease both of these quantities so that the physical width of the distribution and time of the process remain constant (and as well maintaining the ratio $\frac{\delta r^2}{\delta t}$ which determines the physical diffusion constant). Hence, the issues explored in this section pertain to reaching the continuum limit and do not indicate any constraints on the physics of the model.

B. Sub- and superdiffusion from the same model

Finally, with an understanding of the issues involved in taking the continuum limit, we turn to a demonstration of

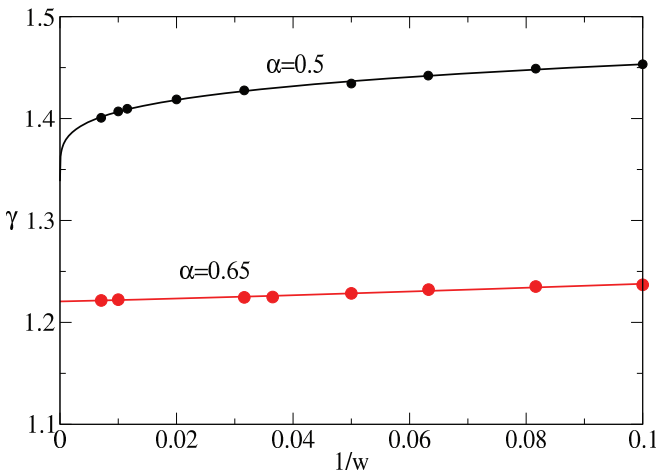


FIG. 4. (Color online) γ as a function of the inverse of the initial width (in lattice units). The lines are fits to $\gamma(w) = a_0 + a_1(1/w)^\alpha$. For $\alpha = 0.5$, the fit gives $\gamma(w \rightarrow \infty) = 1.339$ and for $\alpha = 0.65$, $\gamma(w \rightarrow \infty) = 1.221$. The expected values of γ based on the nonlinear Fokker-Planck equation are $4/3 = 1.333$ and $40/33 = 1.212$, respectively.

sub- and superdiffusion from the same model. To do so, we have to address two additional issues. The first is that the choice $a = 0$ is problematic for subdiffusion. The reason is that if the distribution is zero for, say, $r > r_0$ then with $a = 0$ the probability for a walker to jump from any site $r < r_0$ to a site $r > r_0$ is zero [see Eq. (20)]. Even with an initial condition that, technically, has infinite support (such as a Gaussian), the distribution will be numerically zero outside some range so that in the diffusive case the maximum support is limited. To be able to perform arbitrarily long simulations over arbitrarily large lattices, we must have $a > 0$ in the jump probabilities [Eq. (18)]. The second issue is purely a matter of the choice of problem: we wish to display both subdiffusion and superdiffusion in the same system while changing only a single control parameter. Because the rates of the two processes are very different, the comparison necessitates either very long runs for the subdiffusive process or very restricted ranges of exponents for the superdiffusive process. Our compromise presented here was to take somewhat higher elementary probabilities, $p_n = 10^{-3}$, $n \in [-2, -1, 1, 2]$, $a = 10^{-4}$, and $0.65 \leq \alpha \leq 2$ and begin with an initial Gaussian with width ten lattice units. The results are shown in Fig. 1 where, after an initial transient period, the three regimes of diffusive behavior are clearly visible.

V. CONCLUDING COMMENTS

Beginning with a general formalism for describing the statistics of a population of interacting random walkers developed previously [13,14], we have constructed a particular class of interactions that can give rise to subdiffusion, ordinary diffusion, and superdiffusion with the adjustment of a single parameter. This flexibility depends on the introduction of nonlocal as well as nonlinear interactions between the walkers. Not only does the mean squared displacement show the characteristic behavior of these three regimes, but the systems are diffusive in the strong sense of admitting self-similar solutions. Our model also demonstrates universality: not only does our particular ansatz give the same macroscopic behavior independent of the choice of the parameter a , but the subdiffusive regime reproduces the same nonlinear Fokker-Planck equation as in our previous work that was based on a local interaction [14]. On the other hand, it is worth noting that the self-similar behavior results from self-similar initial conditions: because of the nonlinearity of the generalized diffusion equation, we cannot know whether other initial conditions might evolve into other classes of long time behavior.

We note that our calculations are based on a particular ansatz for the concentration dependence of the jump probabilities, Eq. (13). The ansatz was motivated by simplicity and the requirements on the probabilities such as positivity and normalization. Otherwise, there is nothing special or unique about the choices made here: in particular, the fact that we allow for jumps of length 2 and the form of the ansatz itself. While we were able to characterize the effect of our model in terms of effective attraction or repulsion of the population of walkers, no attempt was made to relate it to microscopic interactions (e.g., particular force laws). Nevertheless, the underlying physics is simply that an effective

repulsion between the walkers gives rise to superdiffusion while an attraction causes subdiffusion. It is the demonstration that such a mechanism can cause anomalous diffusion that is one of the main physical results of this paper. The actual form of the jump probabilities, given in Eq. (18), is irrelevant to establishing this point. The determination of simpler or more physical alternatives to Eq. (18) is a matter for future research.

It is interesting to ask whether the present approach might be related to other mechanisms that generate anomalous diffusion. As discussed in the Introduction, many of these involve non-Markovian elements while here the microscopic random walk has no memory at all: it is simply the interaction between an individual walker and the local concentration of walkers at a particular instant that gives rise to the anomalous behavior. One Markovian mechanism for generating superdiffusion is the Lévy flight in which the probability to make a jump of a given length decays, asymptotically, as a power of the length. This therefore allows for arbitrarily long jumps in one time step. However, even though there is a superficial similarity in the occurrence of power laws in the Lévy flight and our model, the two mechanisms are completely distinct since here the dynamics does not rely on long-ranged jumps. Indeed, in the numerical example presented above, the jumps were limited to at most two lattice sites and we have obtained similar results allowing for only nearest-neighbor jumps. We do not achieve superdiffusion by making jumps of a given length faster or by allowing jumps to be very long during a fixed time (as in the Lévy flight) but by a bias in the direction of a jump that is based on the local density of walkers. So our approach represents a completely independent mechanism for generating anomalous diffusion.

One aspect of the specific model studied here that deserves discussion is the sensitivity to initial conditions. We found that not all initial conditions led to self-similar long-time solutions. One reason for this, as discussed above, is the need to respect the various assumptions necessary to derive the generalized diffusion equation from the microscopic dynamics. However, it is also true that the generalized diffusion equation is nonlinear so that it is not easy to make general statements about its long-time behavior. It is possible that all initial conditions will lead to the same asymptotic state but it is also possible there could be classes of initial conditions that lead to different asymptotic states. It is even possible that the generalized diffusion equation is not ergodic: i.e., that the long-time behavior preserves a memory of the initial condition. Based on numerical experiments beyond those reported here, we do not believe this is the case but a rigorous investigation, e.g., based on Kinchin's theorem such as has been made for the fractional diffusion equation (see [17]), has yet to be attempted.

Another interesting aspect of our results is that the range of scaling exponents that can be generated is restricted to $0 < \gamma \leq 1.5$ [recall that for larger values of γ the mean squared displacement does not exist; see Eq. (29)]. The upper limit is due to the nature of the self-similar solutions which are power laws. As such, they give a finite result only for a finite range of

moments of the spatial variable. Normalization (the existence of a zeroth-order moment) demands that $\alpha \geq -1$, which is not restrictive in terms of the scaling exponent. However, existence of the mean squared displacement itself demands that $\alpha > \frac{1}{3}$, thus giving the quoted limit on γ . In contrast, one typically expects that the upper limit for superdiffusion is $\gamma = 2$, corresponding to ballistic motion. The difference is that ballistic motion is not stochastic: an initial condition of a δ -function concentration of walkers at the origin would evolve, at best, as two δ functions moving in opposite directions at constant speed with the only stochasticity occurring in the initial choice of direction. In contrast, the “free” limit of our model is the case of no interactions corresponding to ordinary diffusion. Moving away from ordinary diffusion requires turning on interactions and there is no reason to expect that this should ever lead to deterministic, nonstochastic behavior. As a matter of fact ballistic motion, although exhibiting mathematically a form corresponding to $\gamma = 2$, originates from a physical mechanism (such as tracer dispersion [2] in an active medium [3]) different from molecular diffusion where free (ballistic) motion occurs at the microscopic scale only in the mean free path regime.

Other models, such as the fractional diffusion equation, which is based on a continuous time random walk with power-law-distributed waiting times, can also give rise to anomalous diffusion. So it is natural to ask the following questions: (i) which approach is appropriate to describe the physics of anomalous diffusion? and (ii) when experimental results are analyzed, how can one discriminate between different approaches in order to establish the underlying mechanism? Our view is that all of the proposed mechanisms are potentially relevant and that different mechanisms may be at work in different physical systems. A more pertinent question is therefore how one might distinguish, experimentally, between the different models. Clearly, since they all produce anomalous diffusion in terms of the mean squared displacement, the test must involve something else. We note, for example, that the probability (or concentration) distribution predicted by the fractional diffusion equation is a stretched exponential [10,11] which is qualitatively quite different from the power-law distributions predicted by the present model. Therefore, a determination of the distribution would be one powerful method for distinguishing between the microscopic mechanisms. Unfortunately, in practice this is more difficult to extract from experiments than is the mean squared displacement and so it is seldom available. One notable exception is a recent experiment on morphogen-gradient generation, where in fact we have shown that the power-law distributions seem to provide a much better description of the data than exponential distributions [15].

ACKNOWLEDGMENT

The work of J.F.L. was supported by the European Space Agency under Contract No. ESA AO-2004-070.

- [1] A. Einstein, *Ann. Phys. (Leipzig)* **17**, 549 (1905).
 [2] See, e.g., T. Sanchez *et al.*, *Nature (London)* **491**, 431 (2012).
 [3] See, e.g., K. M. Douglass, S. Sukhov, and A. Dogariu, *Nat. Photonics* **6**, 834 (2012).

- [4] See, e.g., T. Fujiwara *et al.*, *J. Cell Biol.* **157**, 1071 (2002).
 [5] I. Calvo and R. Sanchez, *J. Phys. A* **41**, 282002 (2008).
 [6] F. Höfling and T. Franosch, *Rep. Prog. Phys.* **76**, 046602 (2013).
 [7] G. M. Schütz and S. Trimper, *Phys. Rev. E* **70**, 045101 (2004).

- [8] N. Kumar, U. Harbola, and K. Lindenberg, *Phys. Rev. E* **82**, 021101 (2010).
- [9] M. A. Desposito, *Phys. Rev. E* **84**, 061114 (2011).
- [10] I. M. Sokolov, J. Klafter, and A. Blumen, *Phys. Today* **55**(11), 48 (2002).
- [11] R. Metzler and J. Klafter, *Phys. Rep.* **339**, 1 (2000).
- [12] E. Barkai, Y. Garini, and R. Metzler, *Phys. Today* **65**(8), 29 (2012).
- [13] J. P. Boon and J. F. Lutsko, *Europhys. Lett* **80**, 60006 (2007).
- [14] J. F. Lutsko and J. P. Boon, *Phys. Rev. E* **77**, 051103 (2008).
- [15] J. P. Boon, J. F. Lutsko, and C. Lutsko, *Phys. Rev. E* **85**, 021126 (2012).
- [16] For an application see Ref. [15].
- [17] S. Bruov, R. Metzler, and E. Barkai, *Proc. Natl. Acad. Sci. U.S.A.* **107**, 13228 (2010).